NASA TECHNICAL NOTE **NASA TN D-7737**

NASA TN D-7737

COMPARISON OF EXPERIMENTAL AND PREDICTED PERFORMANCE OF 150-MILLIMETER-BORE SOLID AND DRILLED BALL BEARINGS TO 3 MILLION DN

by Herbert W. Scibbe and Harold E. Munson

Lewis Research Center
Cleveland, Ohio 44135

NATIONAL AERONAUTICS AND SPACE ADMINISTRATION • WASHINGTON, D. C. • JULY 1974

1. Report No.	2. Government Accession No.	3. Recipient's Catalog No.
NASA TN D-7737		

4. Title and Subtitle
COMPARISON OF EXPERIMENTAL AND PREDICTED PERFORMANCE OF 150-MILLIMETER-BORE SOLID AND DRILLED BALL BEARINGS TO 3 MILLION DN

5. Report Date
JULY 1974

6. Performing Organization Code

7. Author(s)
Herbert W. Scibbe, Lewis Research Center; and Harold E. Munson, Marlin-Rockwell Div. of TRW, Inc., Jamestown, N. Y.

8. Performing Organization Report No.
E-7722

9. Performing Organization Name and Address
Lewis Research Center
National Aeronautics and Space Administration
Cleveland, Ohio 44135

10. Work Unit No.
502-22

11. Contract or Grant No.

12. Sponsoring Agency Name and Address
National Aeronautics and Space Administration
Washington, D.C. 20546

13. Type of Report and Period Covered
Technical Note

14. Sponsoring Agency Code

15. Supplementary Notes

16. Abstract
Seven 150-millimeter-bore ball bearings were run under 8900-newton (2000-lbf) thrust load at speeds from 6670 to 20 000 rpm (1 million to 3 million DN). Four of the bearings had conventional solid balls, and three bearings had drilled (cylindrically hollow) balls with 50-percent mass reduction. The bearings were under-race cooled and slot lubricated with a type II ester oil at flow rates from 4.35×10^{-3} to 5.94×10^{-3} cubic meter/min (1.15 to 1.57 gal/min). Friction torque and temperature were measured on all bearings. While there was considerable spread in the temperature data, the drilled ball bearings tended to run slightly cooler than the solid ball bearings at higher speeds. No significant difference in torque was noted, however, between the solid and drilled ball bearings. One bearing of each type was rerun at 17 800-newton (4000-lbf) thrust load. The solid ball bearings performed satisfactorily at 3 million DN. However, at about 2 million DN the drilled ball bearing experienced a broken ball, and cracks appeared in other balls as a result of flexure fatigue. Metallurgical examination of the cracked balls indicated a brittle structure in the bore of the drilled balls.

17. Key Words (Suggested by Author(s))
Bearings
Ball bearings
Drilled ball
High speed
Flexure fatigue

18. Distribution Statement
Unclassified - unlimited
Category 15

19. Security Classif. (of this report)	20. Security Classif. (of this page)	21. No. of Pages	22. Price*
Unclassified	Unclassified	~~27~~ 29	$3.25

* For sale by the National Technical Information Service, Springfield, Virginia 22151

COMPARISON OF EXPERIMENTAL AND PREDICTED PERFORMANCE OF 150-MILLIMETER-BORE SOLID AND DRILLED BALL BEARINGS TO 3 MILLION DN

by Herbert W. Scibbe and Harold E. Munson*

Lewis Research Center

SUMMARY

Tests were conducted with seven 150-millimeter-bore, angular-contact, split-inner-race ball bearings using either solid balls or drilled balls with a 50-percent mass reduction. Bearings were operated at thrust loads of 8900 and 17 800 newtons (2000 and 4000 lbf) at speeds from 6670 to 20 000 rpm (1 million to 3 million DN) with a type II ester oil as lubricant. A digital computer program was used to predict analytically the performance of the solid and drilled ball bearings over the same range of operating conditions. The analytical and experimental bearing results were then compared.

All seven bearings were run successfully over the speed range at the 8900-newton (2000-lbf) thrust load. Friction torque and outer-race and scavenge-oil temperatures were measured on all bearings. The outer-race and scavenge-oil temperatures of the solid and drilled ball bearings were approximately the same over the speed range. The bearing torques were also compared and found to be approximately the same. However, one drilled ball bearing had torque values that were slightly higher than those of the comparable solid ball bearings, particularly above 15 000 rpm (2.25 million DN).

One solid and one drilled ball bearing were also run at 17 800-newton (4000-lbf) thrust load. The solid ball bearing performed satisfactorily to 3 million DN. However, the drilled ball bearing experienced a broken ball at 2 million DN. Metallurgical examination revealed cracks in two other drilled balls and a brittle structure near the hole bore. It was concluded that the drilled balls failed as the result of flexure fatigue. These ball failures were similar to those reported by another investigator wherein 50-percent-weight-reduction drilled balls were run in 125-millimeter-bore ball bearings at thrust loads to 22 000 newtons (5000 lbf) and speeds to 3 million DN.

Comparison of experimental bearing temperatures and torque with those predicted by the computer program indicated good temperature correlation with both solid and drilled balls at both thrust loads throughout the speed range. However, computed torque values were approximately one-half the measured bearing torque at each speed.

*Marlin-Rockwell Division of TRW, Inc., Jamestown, New York.

INTRODUCTION

Recent trends in gas turbine design and development have been toward engines with higher thrust-weight ratios and increased power output, which result in a requirement for higher shaft speeds and larger shaft diameters (ref. 1). Bearings in current-production aircraft turbine engines operate in the range from 1.5 million to 2 million DN (product of bearing bore in millimeters and shaft speed in rpm). Engine designers anticipate that turbine bearing DN values will have to increase to 2.5 million to 3 million by 1980.

When ball bearings are operated at DN values above 1.5 million, centrifugal forces produced by the balls can become significant. The resulting increase in Hertz stresses at the outer-race ball contacts may seriously shorten bearing fatigue life. The magnitude of the high-speed bearing problem is evident from the curves of figure 1. The solid curves of figure 1 illustrate the effect of DN on the fatigue life of a thrust-loaded 150-millimeter-bore solid ball bearing at two values of thrust load. These curves are based on the high-speed-bearing analysis of reference 2. An increase in speed from a DN value of 1.5 million to 3.0 million results in a theoretical reduction in life by a factor of 20 at the 8900-newton (2000-lbf) thrust load and by a factor of 10 at the 17 800-newton (4000-lbf) thrust load. These are typical thrust loads that a bearing of this bore size would carry in an aircraft turbine engine.

High centrifugal forces are largely responsible for the drastic reduction in predicted fatigue life at high DN values. It is therefore logical to consider methods for reducing the factors that contribute to ball centrifugal loading, such as ball mass, ball orbital speed, and orbital radius. Theory indicates that reductions in ball mass can be quite effective in extending bearing fatigue life at high speeds. The dashed curves of figure 1, when compared with the solid curves, illustrate the theoretical improvement in life with a 50-percent reduction in ball weight. At 3 million DN and 17 800-newton (4000-lbf) thrust load, for example, fatigue life is improved by a factor of 2.5.

Both thin-wall spherically hollow and drilled balls have been evaluated in short-time, high-speed bearing experiments (refs. 3 to 7). The drilled-ball concept, wherein ball mass is reduced as much as 50 percent by machining an accurate concentric hole through the ball, showed particular promise for 3-million-DN bearing applications (refs. 6 and 7)

Drilled balls, as compared with welded hollow balls, have several advantages: (1) fabrication is accomplished by standard ball processes; (2) they can be easily inspected for flaws; (3) hole concentricity can be maintained very accurately, thus alleviating problems of ball unbalance at high speed; and (4) a smooth surface finish can be achieved, without the irregularities present in the weld area of a spherically hollow ball. One disadvantage of drilled balls is that special cages are required, with ball alinement restraints, to prevent the edge of the hole from damaging the race grooves during bearing startup.

This investigation was conducted (1) to experimentally evaluate 150-millimeter-bore ball bearings with conventional solid balls and with drilled balls, using under-race cooling and slot lubrication techniques at speeds to 3 million DN; (2) to compare torque and temperature data of the drilled and solid ball bearings over the same operating conditions; and (3) to compare the experimental torque and temperature data with results obtained analytically from a computer program.

Tests were conducted with 150-millimeter-bore, angular-contact, split-inner-race ball bearings using either solid or drilled balls. The bearings were operated at thrust loads of 8900 and 17 800 newtons (2000 and 4000 lbf) at speeds from 6670 to 20 000 rpm (1 million to 3 million DN). The lubricant was a type II ester oil that met MIL-L-23699 specifications. Under-race cooling and slot lubricating techniques were used throughout the tests. The bearings used 22.2-millimeter (0.875-in.) diameter balls. The drilled balls were made by electric discharge machining a 13.5-millimeter (0.533-in.) diameter hole through the center of a solid ball to effect a 50-percent weight reduction. The drilled-ball cages had ribs machined on opposite sides of each ball pocket to prevent ball misorientation. All tests were conducted at Marlin-Rockwell Division of TRW, Incorporated, Jamestown, New York, under NASA contract NAS3-15343.

APPARATUS AND INSTRUMENTATION

Bearing Test Apparatus

Dynamic testing of the 150-millimeter-bore ball bearing was conducted on the three-bearing test spindle shown schematically in figure 2. A 149-kilowatt (200-hp), 440-volt, three-phase electric motor provided an essentially constant speed of 1750 rpm to the system. An eddy-current clutch provided a variable output speed from near zero to 2000 rpm. The output speed of the clutch was increased by a factor of nearly 15 through a combination of pulleys, belts, and a gearbox.

The test bearing was cantilever mounted on the test spindle, as shown in figure 2. The bearing was mounted on the shaft with a 0.0635-millimeter (0.0025-in.) interference fit. Thrust load was applied to the test bearing by pressurizing a hydraulic cylinder connected to the bearing housing by a 40-centimeter (15.75-in.) length of chain. This method of loading minimized possibilities of misalinement and produced only slight torque tare. The thrust load produced by the hydraulic cylinder was calculated from pressure gage readings. Reaction to the thrust load was provided by an 80-millimeter-bore ball support bearing. This ball bearing and another 80-millimeter-bore ball bearing provided radial support for the shaft. A bearing-preload spring, plus a sliding housing fit for the rear support bearing maintained axial load on the support bearings at all times, thus assuring radial rigidity.

Lubrication System

The lubrication system included a common oil sump with electric heating elements, a supply pump, and a filter. Separate oil supply lines were used for the support bearings and the test bearing. The oil supply to the test bearing was cooled as necessary to maintain a constant oil-inlet temperature of 367 K (200° F). Support bearing oil had an additional cooler to provide lower oil-inlet temperature to the support bearings. All lubricant and coolant for the test bearing entered the test head from the center of the hollow shaft, as shown in figure 2. Oil reached the outer diameter of the shaft near the unloaded half of the inner race, then passed under the inner race through 12 equally spaced axial passages, each 2.38 millimeters (0.0938 in.) deep by 4.78 millimeters (0.188 in.) wide. At the juncture of the two inner-race halves, a portion of the oil was forced, by centrifugal force, into the bearing through the radial passages at the interface. The remaining oil passed on to the end of the axial passages and was discharged separately. During actual testing, most of the oil entered the bearing. Multiple oil-outlet holes were provided on each side of the bearing housing for lubricant scavenge. Multiple holes were also provided for cooling-oil scavenge. The several oil-outlet passages were manifolded, and the oil was then pumped back to the sump. Oil-inlet and oil-outlet flow rates were measured by volumetric-type flowmeters. Oil flowmeters were installed in suction lines to the scavenge pump. A type II ester oil that met MIL-L-23699 specifications was used. The viscosity was 5.5×10^{-3} N-sec/m^2 (0.8×10^{-6} lbf-sec/in.^{2}) at 367 K (200° F). Oil flows ranged from 4.35×10^{-3} to 5.94×10^{-3} cubic meter per minute (1.15 to 1.57 gal/min).

Instrumentation

Temperature measurement. - Temperatures were measured by Chromel-Alumel thermocouples and recorded on millivolt strip-chart recorders. Temperatures were measured at the following locations:

(1) Oil inlet, the center of the hollow shaft

(2) Test bearing outer ring

(3) Oil outlet on the inboard side of the test housing

(4) Oil outlet on the outboard side of the test housing

(5) Oil outlet for test bearing under-race cooling oil

(6) Oil sump

(7) Oil at input flowmeter to test bearing

(8) Outer rings of both support bearings

Individual oil-outlet temperatures were measured in lines from the test bearing which came out at the six o'clock positions, and thermocouples were located 5.1 to 7.6

centimeters (2 to 3 in.) from the bearing. All bearing and oil temperatures were accurate to within ±1 K (±2° F) of the indicated readings.

Flow-rate measurement. - Oil flows were measured by volumetric-type flowmeters. The flowmeter measuring oil to the test bearing was calibrated with 367 K (200° F) test oil. Oil-outlet flowmeters were used as indicators, and actual measurements of scavenge flows were made by periodically bypassing them, one at a time, into a graduated cylinder. Overall accuracy of the volumetric flow measurements was $\pm 2 \times 10^{-4}$ cubic meter per minute (±0.2 liter/min) at constant temperature.

The torque of the test bearing was measured by using a strain gage mounted on the restraining arm. The strain-gage signal was amplified and recorded. This force, multiplied by the length of the torque arm, constituted the torque. Oil-outlet lines, while flexible, provided a small tare torque.

Speed was measured by a magnetic pickup which sensed passage of a small hole in the spindle pulley. The signal was indicated by a frequency counter reading in revolutions per second. Basic accuracy of the speed measurement was ±1 hertz or ±60 rpm.

TEST BEARINGS

The test bearing specifications are listed in table I. The bearings were 150-millimeter-bore, angular-contact, split-inner-race ball bearings with 22.2-millimeter (0.875-in.) diameter balls. The one-piece machined cages were located on the outer race. The bearings with one-half of the inner race removed are shown in figure 3. In each mating face of the inner-race halves, there were 12 radial slots of 1.3-millimeter (0.050-in.) radius extending from the bore to the raceway. The specifications for the conventional solid and drilled ball bearings were identical except for the holes in the drilled balls and a modification made to the drilled-ball cage.

Drilled-Ball Design

A section view of the drilled ball showing details is presented in figure 4. A matched set of 23 balls, Anti-Friction Bearing Manufacturers Association (AFBMA) grade 10, were selected for each drilled ball bearing. Parallel flats 16.84 millimeters (0.663 in.) apart were ground on each ball. A 13.4-millimeter (0.527-in.) diameter concentric hole was electric discharge machined (EDM) through each ball. The hole was then ground to 13.54-millimeter (0.533-in.) diameter with a 0.41-micrometer rms (16-μin. rms) finish. Concentricity with the ball outer diameter was maintained to within 0.020 millimeter (0.0008 in.). The hole diameter of 13.54 millimeters (0.533 in.) resulted in a weight reduction of approximately 50 percent from that of a solid ball.

Drilled-Ball Cage Design

The cage design for the drilled ball bearings was the same one-piece design as that used for the solid ball bearings, with one exception. The drilled-ball cage had integral ribs machined into opposite sides of each ball pocket, as illustrated in figure 5. These ribs restricted twisting movement of the ball to about 37° and prevented the edge of the hole from riding on the race groove during bearing operation. The ribs also restricted ball spin about a vertical axis. All cages were made from SAE 4340 steel. After silver plating, they were balanced to within 3 gram-centimeters (0.04 oz-in.).

PROCEDURE

Test Procedure

Each bearing was installed in the test housing so that the puller-groove half of the inner race was on the load mechanism side. Lubricating oil was preheated and pumped through the test apparatus. Approximately 4450-newton (1000-lbf) thrust load was applied to the stationary test bearing.

The test apparatus was started and allowed to run at 3000 rpm while the drive, load, and lubrication systems and the instrumentation were checked. When no irregularities were noted, the load was increased to the test value, either 8900 or 17 800 newtons (2000 or 4000 lbf), and the speed was increased to 6670 rpm.

The test apparatus was run at 6670 rpm and the scheduled load until the oil-inlet temperature was stabilized at 367 ± 2 K ($200^{\circ}\pm3^{\circ}$ F). The apparatus was then run for a period of at least 10 minutes, during which time the difference between the oil-inlet and bearing outer-race temperatures did not vary more than 1 K (2° F). Instrument readings were recorded during this time.

This procedure was repeated at shaft speeds of 10 000, 13 330, 15 000, 16 670, 18 330, and 20 000 rpm. During the first three tests of the solid-ball test bearings, the oil flow rate was increased to 40 percent of the flowmeter capacity after completion of a 15 000-rpm datum point. In the remaining tests the oil flow rate was increased to 40 percent of capacity after completion of the 13 330-rpm datum point.

In a few tests it was necessary to stop temporarily because of equipment malfunction. When testing was resumed, shaft speed was increased through previously accomplished datum points without waiting for absolute temperature stabilization, but comparisons were made to assure basic agreement. Formal testing was renewed at the next scheduled datum point.

Scavenge-oil flows were measured by bypassing the flow into a graduated cylinder and using a stopwatch. Duration of the flow check was 10 to 15 seconds. At least two checks were made for each datum point for each flow. After the bypass line was opened for each check, the flow was permitted to stabilize before measurements were taken. The accuracy of these manual measurements is within ±5 percent.

Analytical Procedure

A computer program (ref. 2) was used to calculate, under elastohydrodynamic (EHD) lubrication conditions, the bearing temperatures, torque, heat generation, maximum Hertz stresses, and fatigue life of the 150-millimeter-bore ball bearings used in this investigation. Computations were made for both solid and drilled ball bearing configurations (table I) over the range of operating speeds to 3 million DN at thrust loads of 8900 and 17 800 newtons (2000 and 4000 lbf) with oil flow rates of 4.35×10^{-3} and 5.80×10^{-3} cubic meter per minute (1.15 and 1.53 gal/min). The computed values for bearing temperature and torque at both thrust loads were then plotted and compared with the experimental data.

The bearing oil-inlet temperature that was used for the computer program input at each speed differed from the experimental constant value of 367 K (200° F) to account for heat gain by the oil for each speed increment. Therefore, for each 3330-rpm (0.5 million DN) increment above 6670 rpm the oil temperature was increased 5.5 K (10° F), so that at the maximum shaft speed of 20 000 rpm (3 million DN) the oil-inlet temperature value used was 389 K (240° F).

The bearing thermal model used in the computer program (ref. 2) was based on the frictional heat generated within the bearing, the amount of lubricant within the bearing cavity, and the flow rate of lubricant through the bearing. The major sources of bearing heat generation were (1) the sliding motion at the ball-raceway contacts, (2) the viscous drag caused by the balls plowing through the lubricant, and (3) the viscous drag of the cage rails sliding over the piloted race lands. Heat was dissipated from the bearing-shaft-housing system through conduction, convection, and radiation heat-transfer modes. For each bearing operating condition, 31 temperatures were defined for the bearing-shaft-housing system. For purposes of this investigation the temperatures of particular interest were the bearing outer-race temperature, the oil-inlet temperature, and the scavenge-oil outlet temperatures (fig. 2).

RESULTS AND DISCUSSION

Results of Tests on Solid and Drilled Ball Bearings

Tests at 8900-newton (2000-lbf) thrust load. - The results of tests on the conventional solid ball bearings 162A, 433A, 384A, and 398A at 8900-newton (2000-lbf) thrust load and speeds from 6670 to 20 000 rpm (1 million to 3 million DN) are presented in table II. The running time, oil-inlet temperature and flow, scavenge-oil temperatures (from both the loaded and unloaded halves of the inner race), outer-race temperature, and bearing torque are shown for each shaft speed.

In preliminary apparatus shakedown tests, oil flow rates from 4×10^{-3} to 6×10^{-3} cubic meter per minute (1 to 1.5 gal/min) were approximated as sufficient to lubricate and cool the test bearing at 8900-newton (2000-lbf) thrust load at speeds to 19 500 rpm. For the bearings in the test program, at an inlet temperature of 367 K (200° F), an actual flow rate of 4.35×10^{-3} cubic meter per minute (1.15 gal/min) was used at speeds to 15 000 rpm, and a flow rate of 5.80×10^{-3} cubic meter per minute (1.53 gal/min) was used at speeds above 15 000 rpm.

Bearing 433A ran considerably cooler than either bearing 384A or 398A and slightly warmer than bearing 162A. The scavenge-oil temperatures measured at the loaded and unloaded halves of the split inner race of bearing 433A indicated a higher temperature from the loaded side, varying from 4 K (8° F) higher at 6670 rpm to as much as 24 K (43° F) higher at 20 000 rpm (fig. 2 and table II). Additionally, scavenge-oil temperatures on the loaded inner-race side measured more than 10 K (18° F) higher than bearing outer-race temperatures at the two highest shaft speeds. Maximum torque measured for bearing 433A was 9.49 newton-meters (84 lbf-in.) at 20 000 rpm.

Data for the three drilled ball bearings (429A, 377A, and 230A) are presented in table III. The bearings were run under the same conditions as were the solid ball bearings, and all three operated satisfactorily through 20 000 rpm (3 million DN).

Scavenge-oil temperatures for the three drilled ball bearings (table III) from the loaded half of the inner-race were from 12 to 25 K (21° to 45° F) higher than temperatures from the unloaded half at speeds from 15 000 to 20 000 rpm. These scavenge-oil temperatures were also higher than the bearing outer-race temperatures by approximately 11 K (20° F) at 20 000 rpm. The scavenge-oil temperatures for these three drilled ball bearings were similar to those recorded for bearing 433A (table II), the only solid ball bearing that operated normally throughout the speed range.

Outer-race temperatures for solid ball bearing 433A and drilled ball bearing 377A are plotted as a function of shaft speed in figure 6(a). The drilled ball bearing had slightly lower temperatures than did the solid ball bearing throughout the speed range. Bearing torque as a function of shaft speed for bearings 433A and 377A is shown in figure 6(b). Torque values for the solid ball bearing are somewhat lower than those for the drilled ball bearing throughout the speed range. The change in slope indicated at 15 000 rpm on the temperature and torque plots for both bearings is probably the result of the increase in oil flow at this speed.

Tests at 17 800-newton (4000-lbf) thrust load. - Solid ball bearing 433A and drilled ball bearing 377A were selected for testing at the 17 800-newton (4000-lbf) thrust load. The test data are presented in table IV, and the bearing outer-race temperature and torque are plotted as a function of shaft speed in figure 7. The time at speed shown in tables II to IV is the bearing running time in minutes at that indicated speed, after a temperature equilibrium condition had been attained in the bearing. The same oil flows as in the 8900-newton (2000-lbf) load tests were used. Solid ball bearing 433A ran successfully throughout the speed range. Bearing torque and temperature were significantly higher at each speed than in the lower load test. Drilled ball bearing 377A ran successfully at the two lower speed settings, but experienced a broken ball after running for 6 minutes at 13 000 rpm. Failure was indicated by a high and erratic torque accompanied by a rapidly increasing temperature. Seizure did not occur, however, and the bearing was operated for a short time at reduced speed and load before the test was terminated.

Comparison of Bearing Experimental and Analytical Results

The computed results for both a solid and a drilled ball bearing at 8900- and 17 800-newton (2000- and 4000-lbf) thrust loads are given in table V. Examination of table V shows that the outer-race temperature, scavenge-oil temperature, and bearing torque values are approximately the same for both the solid and drilled ball bearings for any given speed and load condition.

Bearing temperature and torque. - The computed bearing outer-race and scavenge-oil temperatures of table V were compared with the experimental temperature values at 8900-newton (2000-lbf) (tables II and III) and 17 800-newton (4000-lbf) thrust loads (table IV). The computer values are slightly lower for both solid and drilled ball bearings at all speeds, except 20 000 rpm. At 20 000 rpm the computed temperatures are a few degrees higher. Computed outer-race temperatures for solid and drilled bearings at both 8900- and 17 800-newton (2000- and 4000-lbf) loads are plotted in figures 6(a) and 7(a), respectively, for comparison with experimental data from solid ball bearing 433A and drilled ball bearing 377A.

Computed bearing torque values shown in table V are less than one-half the experimental values at both thrust loads. Computed torque values at 8900-newton (2000-lbf) load are plotted in figure 6(b) and compared with data for bearings 433A and 377A. Computed and experimental torque values at 17 800-newton (4000-lbf) load are compared in figure 7(b). Although the computed torque values did not agree with experimental data for these bearings, the computed temperature data did show good correlation with actual bearing temperatures for both thrust loads. Therefore, it was concluded that the computer program was a useful tool for predicting operating temperatures of 150-millimeter-bore ball bearings over a range of operating conditions.

Maximum Hertz compressive stress. - The maximum Hertz compressive stresses at 20 000 rpm (3 million DN) for the 8900-newton (2000-lbf) thrust load were 1138×10^6 N/m^2 (165 000 psi) at the inner race and 1413×10^6 N/m^2 (205 000 psi) at the outer race for the solid ball bearing. At the 17 800-newton (4000-lbf) load these stresses increased to 1331×10^6 N/m^2 (193 000 psi) at the inner-race contact and to 1579×10^6 N/m^2 (229 000 psi) at the outer-race contact. For the drilled ball bearing, the inner-race stresses remained essentially the same as those determined for the solid ball bearing. However, the stress at the outer-race contact was reduced about 16 percent for the 8900-newton (2000-lbf) load and 14 percent for the 17 800-newton (4000-lbf) load from the values with the solid balls.

Bearing Post-Test Inspection

Solid ball bearings. - All four solid ball bearings were visually examined after the 8900-newton (2000-lbf) load tests. Bearings 162A, 384A, and 433A were found to be similar in appearance. The races varied in color from bright and unchanged to a light straw color on the load side. The balls were straw colored. The outer diameter of the cages had two lightly polished rings where contact was made with the outer-race lands. Cage ball-pocket polishing was normal with a shiny band in the silver plating around the periphery of each pocket. Bearing 384A also had shiny bands around each ball; and the outer race had a shiny ball track at its center as a result of a high-speed, no-load condition encountered at the end of the test.

The fourth bearing, 398A, had run hottest of the solid ball bearings. The races and the cage were brown colored and the balls had a bluish tinge. The cage outer diameter showed two polished bands in the silver plating where contact was made with the outer race, with heavier polishing on the inner-race load side. Ball-pocket polishing was similar to that for the other three bearings.

Bearing 433A was also examined after the 17 800-newton (4000-lbf) load test. All components were a darker straw color, and the ball tracks on the races were better delineated than in the lower load test. Figure 8 shows bearing 433A with the inner race removed after the 17 800-newton (4000-lbf) load test. The ball-pocket and outer-locating-surface cage wear can be seen.

Drilled ball bearings. - The three drilled ball bearings were similar in appearance to solid ball bearing 433A after the 8900-newton (2000-lbf) load test. The cage ball pockets indicated light contact between the edges of the balls and the ends of the machined ribs on both sides of each pocket. It appears that contact occurred during bearing start-up, when the balls had oriented themselves.

The results of the drilled ball bearing tests demonstrated that the integrally machined ribs in the cage ball pockets were effective in restricting ball spin about a vertical axis and twisting about a horizontal axis. The ribs also minimized contact of the ball hole edge with the races. It was estimated that this ribbed-cage pocket design was as effective in restricting ball motion during bearing operation as the designs described in references 5 and 6. Furthermore, the ribs could be machined in the ball pockets for a significantly lower cost than either of the other two designs.

Bearing 377A after testing is shown in figure 9. Ball-pocket and outer-locating-surface cage wear and a fractured drilled ball that had broken into two pieces can be seen. All cage pockets show heavy contact between the edges of the balls and the machined ribs in the cage pockets. It was assumed that some bearing instability occurred after the ball failure, and that the heavy contact resulted. However, in no case was the silver plating ruptured.

Drilled-ball contact with the cylindrical surfaces of the cage pockets formed a different wear-band pattern than that created by conventional solid balls. Contact between the solid balls and their pockets formed a uniform wear band around the periphery at the center. Drilled-ball contact on the cage pockets was heaviest at the fore and aft positions because of the restricted ball-spin arc. This wear phenomenon resulted in an edge effect at the ends of the wear band, with ridges impressed into the silver plating. The cage outer surface and drilled-ball contact areas, shown in the closeup view of figure 10, appeared about the same as after the lower load test. The loaded half of the inner race showed a more pronounced ball track than was evident after the lower load test. An additional nick and some scratches were also apparent. The outer race was somewhat scored by the broken ball. The balls showed minor surface distress as a result of running over the roughened outer race. Two balls, in addition to the one that was broken, had cracks in the bores.

Metallurgical examination of drilled balls. - Examination of the broken ball in figure 9 revealed an area of shallow pits in the bore which resulted from inadequate cleanup of the EDM surface. It appeared possible that the fracture might have initiated from a pit, but abrasion resulting from bearing operation for a short time after the initial indication of failure had removed any evidence thereof.

Visual examination of the other 22 drilled balls of bearing 377A indicated that 16 had pits in the bore. Figure 11 is a magnified half-section view of a drilled ball showing the pitted bore surface. At the top of figure 11 cracks are shown that originate at the hole edge and extend axially into the ball. Closer visual examination of the hole edge revealed that several of these cracks had penetrated radially into the ball matrix, as deep as 0.64 millimeter (0.025 in.). A metallographic section of a drilled ball normal to the hole axis is shown in figure 12. Radial cracks and a light-colored, heat-affected zone that extends radially into the ball matrix a maximum of 0.3 millimeter (0.012 in.) from the hole edge can be seen. Microhardness measurements were made on this section and were translated in Rockwell C hardness readings. The Rockwell C hardness values are shown in the enlarged view in the upper left of figure 12 and indicate that the structure of the heat-affected zone was brittle untempered martensite. It was therefore concluded that the AISI M-50 material adjacent to the hole surface had overheated and rehardened during the EDM operation. A region of the ball outside of the heat-affected zone revealed a more normally tempered martensitic structure, as shown in the photomicrograph in the upper right of figure 12. A Rockwell C hardness of 61 for this region is indicated, which is within the range of hardness values specified for the balls in table I.

Ball fractures were also reported in reference 7, wherein 125-millimeter-bore drilled ball bearings were run under conditions similar to those in this investigation. In one bearing a drilled ball had fractured during a run at 2.8 million DN at 13 300-newton (3000-lbf) thrust load. In another bearing run at 2.6 million DN and 22 200-newton (5000-lbf) thrust load, 11 of 21 drilled balls had failed. The ball fractures were similar to that shown for bearing 377A in figure 9. Electron fractographic analysis of the broken balls in reference 7 revealed that a fatigue crack had originated near the hole bore and had propagated to the ball outer surface. It was concluded, therefore, that the drilled balls (ref. 7) had failed due to flexure fatigue.

In reference 8 a finite element analysis was utilized to determine the type and magnitude of the stresses in the drilled balls of reference 7. This analysis showed that a large cycling stress occurs in the bore of the ball as the ball rotates through one revolution under Hertzian loading at 3 million DN. The maximum tangential stress with 22 000-newton (5000-lbf) thrust load ranged from 470×10^6 N/m^2 (70 000 psi) in tension to about 150×10^6 N/m^2 (20 000 psi) in compression, which is a change in stress of 620×10^6 N/m^2 (90 000 psi) and is considered more than adequate to produce flexure fatigue failures in the drilled ball. The balls in this investigation were subjected to the same type of cyclic stress of a lower magnitude, and it is assumed that they also failed in flexure fatigue.

SUMMARY OF RESULTS

Tests were conducted with 150-millimeter-bore, angular-contact, split-inner-race ball bearings using either solid balls or drilled balls with a 50-percent mass reduction. Bearings were operated at thrust loads of 8900 and 17 800 newtons (2000 and 4000 lbf) at speeds from 6670 to 20 000 rpm (1 million to 3 million DN) with a type II ester oil as lubricant. A digital computer program was used to determine, analytically, the performance of the solid and drilled ball bearing designs over the same operating conditions. The investigation provided the following significant results:

1. All seven bearings were run successfully over the speed range at the 8900-newton (2000-lbf) load. The friction torque and the outer-race and scavenge-oil temperatures were measured on all bearings. The three drilled ball bearings tended to run a few degrees cooler than the solid ball bearings, especially at the higher speeds. However, no significant difference in torque data was noted.

2. A solid ball bearing, rerun at 17 800-newton (4000-lbf) load, performed satisfactorily at 3 million DN. At approximately 2 million DN the drilled ball bearing experienced a broken ball. Examination revealed cracks in two other balls that were considered the result of flexure fatigue. Metallurgical examination of these balls revealed a brittle structure in the hole bore.

3. Comparison of the experimental temperature and torque data of the solid and drilled ball bearings with those values determined analytically from a computer program indicated good temperature correlation at all speeds. However, the measured bearing torques were more than twice the computed values.

Lewis Research Center,
National Aeronautics and Space Administration,
Cleveland, Ohio, April 29, 1974,
502-22.

REFERENCES

1. Brown, P. F.: Discussion to Paper Previously Published in ASLE Trans. ASLE Trans., vol. 12, no. 3, Jul. 1969, pp. 204-205.

2. Crecelius, W. J.; and Harris, T. A.: Ultra-High Speed Ball Bearing Analysis. SKF Industries, Inc. (NASA CR-120837), 1971.

3. Coe, Harold H.; Parker, Richard J.; and Scibbe, Herbert W.: Evaluation of Electron-Beam-Welded Hollow Balls for High-Speed Ball Bearings. J. Lub. Tech., vol. 93, no. 1, Jan. 1971, pp. 47-59.

4. Coe, Harold H.; Scibbe, Herbert W.; and Parker, Richard J.: Performance of 75-Millimeter-Bore Bearings to 1.8 Million DN with Electron-Beam-Welded Hollow Balls. NASA TN D-5800, 1970.

5. Coe, Harold H.; Scibbe, Herbert W.; and Anderson, William J.: Evaluation of Cylindrically Hollow (Drilled) Balls in Ball Bearings at DN Values to 2.1 Million. NASA TN D-7007, 1971.

6. Holmes, P. W.: Evaluation of Drilled-Ball Bearings at DN Values to Three Million. I - Variable Oil Flow Tests. NASA CR-2004, 1972.

7. Holmes, P. W.: Evaluation of Drilled-Ball Bearings at DN Values to Three Million. II - Experimental Skid Study and Endurance Tests. NASA CR-2005, 1972.

8. Coe, Harold H.; and Lynch, John E.: Analysis of Stresses at the Bore of a Drilled Ball Operating in a High-Speed Bearing. NASA TN D-7501, 1973.

TABLE I. - SPECIFICATIONS FOR 150-MILLIMETER-BORE BALL BEARINGS

[Bearings were made to Annular Bearing Engineers Committee grade 5 tolerances.]

Rings and balls	
Material	Consumable-electrode, vacuum-melted AISI M-50 steel
Hardness	Rockwell C 60 to 63
Inner-race bore, mm (in.)	150 (5.9053)
Outer-race outside diameter, mm (in.)	225 (8.8583)
Width, mm (in.)	35 (1.3780)
Number of balls	23
Ball outside diameter, mm (in.)	22.225 (0.875)
Pitch diameter, nominal, mm (in.)	186.89 (7.3578)
Contact angle, nominal, rad (deg)	0.5236 (30)
Radial clearance under 147-N (33-lbf) load, mm (in.)	0.107 to 0.142 (0.0042 to 0.0056)
Inner-race radius, percent of ball diameter	52
Outer-race radius, percent of ball diameter	51
Cage	
Material	SAE 4340 steel, silver plated 0.025 to 0.051 mm (0.001 to 0.002 in.) thick per AMS-2412
Hardness	Rockwell C 28 to 32
Cage width, maximum, mm (in.)	28.14 (1.108)
Ball-pocket clearance, diametral, mm (in.)	0.635 to 0.838 (0.025 to 0.033)
Cage-land clearance, diametral, mm (in.)	1.02 (0.040)

TABLE II. - RESULTS FOR 150-MILLIMETER-BORE SOLID BALL BEARINGS

TESTED AT 8900-NEWTON (2000-lbf) THRUST LOAD

Shaft speed, rpm	Product of bearing bore and shaft speed, DN, mm × rpm	Time at speed, min	Oil-inlet temperature		Oil-inlet flow		Scavenge-oil temperature				Outer-race temperature		Bearing torque	
							Unloaded inner race		Loaded inner race					
			K	°F	m^3/min	gal/min	K	°F	K	°F	K	°F	N-m	lbf-in.
Bearing 162A														
6 670	1.00×10^6	180	365	197	4.35×10^{-3}	1.15	---	---	---	---	393	248	5.83	51.6
10 000	1.50	78	365	197	4.35	1.15	411	280	421	298	415	288	5.83	51.6
13 300	2.00	24	369	204	4.35	1.15	436	325	445	342	441	334	5.83	51.6
15 200	2.25	15	372	210	4.65	1.23	450	350	457	363	455	360	6.51	57.6
16 660	2.50	9	372	210	5.80	1.53	445	341	461	370	461	370	7.19	63.6
18 330	2.75	3	358	185	5.80	1.53	449	348	467	381	466	379	7.32	64.8
20 000	3.00	1.2	356	181	5.80	1.53	449	348	467	381	473	391	8.54	75.6
Bearing 433A														
6 670	1.00×10^6	63	366	199	4.35×10^{-3}	1.15	389	241	394	249	391	244	3.72	32.9
10 000	1.50	19.8	366	199	4.35	1.15	416	290	422	300	416	290	4.66	41.2
13 330	2.00	19.8	366	199	4.35	1.15	435	323	452	354	445	342	6.28	55.6
15 000	2.25	90	365	197	5.80	1.53	445	341	463	373	454	358	7.67	67.9
16 670	2.50	21	365	197	5.80	1.53	453	355	472	390	464	375	8.36	74.0
18 330	2.75	33	365	197	5.80	1.53	466	380	492	425	480	405	9.07	80.3
20 000	3.00	21	366	199	5.95	1.57	479	403	503	446	492	426	9.49	84.0
Bearing 384A														
6 670	1.00×10^6	96	367	200	4.35×10^{-3}	1.15	388	238	399	258	395	252	4.88	43.2
10 000	1.50	84	367	200			396	254	426	308	424	304	5.11	45.2
13 330	2.00	42	367	200			406	272	461	370	452	354	5.58	49.4
15 000	2.25	30	365	198			417	291	486	415	478	400	6.28	55.6
15 000	2.25	30	367	200	5.80	1.53	---	---	---	---	463	373	7.45	65.9
16 670	2.50	27	367	200			416	290	483	410	473	392	6.97	61.7
18 330	2.75	42	366	199			428	310	504	448	494	430	8.84	78.2
20 000	3.00	12	366	199			---	---	---	---	512	462	9.99	88.4
Bearing 398A														
6 670	1.00×10^6	81	366	199	4.35×10^{-3}	1.15	375	215	404	268	395	252	----	----
10 000	1.50	48	365	198			386	236	449	348	434	322	----	----
13 330	2.00	81	365	198			400	260	486	415	468	382	----	----
15 000	2.25	15	366	199			411	280	509	457	489	421	----	----
15 000	2.25	18	368	203	5.80	1.53	---	---	508	454	483	409	----	----
16 670	2.50	18	368	203			---	---	523	482	499	438	----	----
18 330	2.75	21	367	200			---	---	545	522	516	470	----	----
20 000	3.00	18	367	200			---	---	578	580	544	519	----	----

TABLE III. - RESULTS FOR 150-MILLIMETER-BORE DRILLED BALL BEARINGS

TESTED AT 8900-NEWTON (2000-lbf) THRUST LOAD

Shaft speed, rpm	Product of bearing bore and shaft speed, DN, mm × rpm	Time at speed, min	Oil-inlet temperature		Oil-inlet flow		Scavenge-oil temperature				Outer-race temperature		Bearing torque	
							Unloaded inner race		Loaded inner race					
			K	°F	m^3/min	gal/min	K	°F	K	°F	K	°F	N-m	lbf-in.
Bearing 429A														
6 670	1.00×10^{6}	48	365	197	4.35×10^{-3}	1.15	389	241	390	242	390	242	3.25	28.8
10 000	1.50	42	366	199	4.35	1.15	411	281	415	288	411	281	5.70	50.4
13 330	2.00	36	366	199	4.35	1.15	433	320	445	342	439	330	6.40	56.6
15 000	2.25	27	367	200	5.80	1.53	445	342	457	363	450	350	7.91	70.0
16 670	2.50	21	366	199	↓	↓	456	362	469	385	461	370	7.91	70.0
18 330	2.75	20	367	200	↓	↓	469	385	486	416	478	400	8.36	74.0
20 000	3.00	21	366	199	↓	↓	483	410	503	445	491	425	10.24	90.6
Bearing 377A														
6 670	1.00×10^{6}	57	365	197	4.35×10^{-3}	1.15	391	245	394	249	391	245	5.42	48.0
10 000	1.50	27	367	200	4.35	1.15	414	285	414	285	414	286	6.78	60.0
13 330	2.00	30	366	199	4.35	1.15	429	312	438	329	432	318	7.19	63.6
15 000	2.25	30	365	197	5.80	1.53	433	320	455	359	447	345	10.85	96.0
16 670	2.50	27	↓	↓	↓	↓	447	345	466	379	455	360	11.53	102.0
18 330	2.75	27	↓	↓	↓	↓	450	350	477	399	466	379	12.20	108.0
20 000	3.00	24	↓	↓	↓	↓	464	375	489	420	478	400	12.20	108.0
Bearing 230A														
6 670	1.00×10^{6}	54	365	197	4.35×10^{-3}	1.15	(a)	---	399	259	396	254	8.14	72.0
10 000	1.50	90	366	199	4.35	1.15	(a)	---	423	302	421	298	8.14	72.0
13 330	2.00	54	367	200	4.35	1.15	(a)	---	445	342	438	328	9.09	80.4
15 000	2.25	69	366	199	5.80	1.53	430	315	444	340	437	327	9.90	87.6
16 670	2.50	21	366	199	↓	↓	440	333	457	363	449	348	10.44	92.4
18 330	2.75	21	365	197	↓	↓	449	348	468	382	457	363	11.53	102.0
20 000	3.00	21	366	199	↓	↓	456	362	479	402	467	381	12.20	108.0

[a]Temperature not recorded.

TABLE IV. - RESULTS FOR SOLID AND DRILLED 150-MILLIMETER-BORE BALL BEARINGS

TESTED AT 17 800-NEWTON (4000-lbf) THRUST LOAD

Shaft speed, rpm	Product of bearing bore and shaft speed, DN, mm × rpm	Time at speed, min	Oil-inlet temperature		Oil-inlet flow		Scavenge-oil temperature				Outer-race temperature		Bearing torque	
							Unloaded inner race		Loaded inner race					
			K	°F	m^3/min	gal/min	K	°F	K	°F	K	°F	N-m	lbf-in.
Bearing 433A														
6 670	1.00×10^{6}	51	365	198	4.50×10^{-3}	1.19	393	248	396	254	395	252	6.37	56.4
10 000	1.50	120	365	198	4.50	1.19	423	302	425	305	427	309	10.85	96.0
13 330	2.00	48	365	198	4.50	1.19	451	352	458	365	460	368	12.20	108.0
15 000	2.25	21	366	199	5.80	1.53	455	360	468	382	471	388	13.02	115.2
16 670	2.50	24	367	200			461	370	488	418	486	415	14.64	129.6
18 330	2.75	27	367	200			478	400	512	462	509	457	15.87	140.4
20 000	3.00	18	367	200			491	424	523	482	521	479	17.63	156.0
Bearing 377A														
6 670	1.00×10^{6}	69	365	198	4.50×10^{-3}	1.19	395	252	397	255	395	252	11.12	98.4
10 000	1.50	18	365	198	4.50	1.19	422	300	425	302	422	300	10.85	96.0
13 000	2.00	6	365	198	4.50	1.19	---	---	---	---	---	---	16.27	144.0

TABLE V. - COMPUTED TEMPERATURES AND TORQUES FOR SOLID AND DRILLED 150-MILLIMETER-BORE BALL BEARINGS

FROM 1 MILLION TO 3 MILLION DN AT 8900- AND 17 800-NEWTON (2000- AND 4000-lbf) THRUST LOADS

Shaft speed, rpm	Product of bearing bore and shaft speed, DN, mm × rpm	Oil-inlet temperature		Oil-inlet flow		Solid ball bearing						Drilled ball bearing					
						Outer-race temperature		Scavenge-oil temperature		Torque		Outer-race temperature		Scavenge-oil temperature		Torque	
		K	°F	m^3/min	gal/min	K	°F	K	°F	N-m	lbf-in.	K	°F	K	°F	N-m	lbf-in.
8900-Newton (2000-lbf) thrust load																	
6 670	1.00×10^6	367	200	4.35×10^{-3}	1.15	389	240	385	234	2.26	20.0	389	241	385	234	2.16	19.1
10 000	1.50	372	210			409	276	408	274	3.48	30.8	410	284	408	274	3.34	29.6
13 330	2.00	378	220			434	321	434	322	4.36	38.6	438	333	435	323	4.26	37.7
15 000	2.25	380	225			449	349	450	351	4.66	41.2	454	358	450	350	4.59	40.6
15 000	2.25	380	225	5.80	1.53	441	335	440	332	4.88	43.2	450	350	441	334	4.80	42.5
16 670	2.50	383	230			455	359	454	357	5.14	45.5	464	375	455	360	5.05	44.7
18 330	2.75	386	235			473	391	472	390	5.56	49.2	481	406	472	390	5.47	48.4
20 000	3.00	389	240			500	441	501	442	6.24	55.2	511	461	501	443	6.19	54.8
17 800-Newton (4000-lbf) thrust load																	
6 670	1.00×10^6	367	200	4.35×10^{-3}	1.15	393	248	389	240	2.70	23.9	394	249	389	240	2.63	23.3
10 000	1.50	372	210			414	286	411	280	3.86	34.2	414	286	410	277	3.68	32.6
13 330	2.00	378	220			437	327	436	325	4.79	42.4	439	331	435	323	4.60	40.7
15 000	2.25	380	225			451	352	450	351	5.21	46.1	452	354	448	347	5.03	44.5
15 000	2.25	380	225	5.80	1.53	443	337	439	330	5.45	48.2	444	340	437	327	5.24	46.4
16 670	2.50	383	230			455	360	452	354	5.82	51.5	457	362	450	350	5.62	49.7
18 330	2.75	386	235			471	389	470	386	6.51	57.6	475	395	467	382	6.25	55.3
20 000	3.00	389	240			496	434	496	433	7.34	65.0	500	441	493	427	7.14	63.2

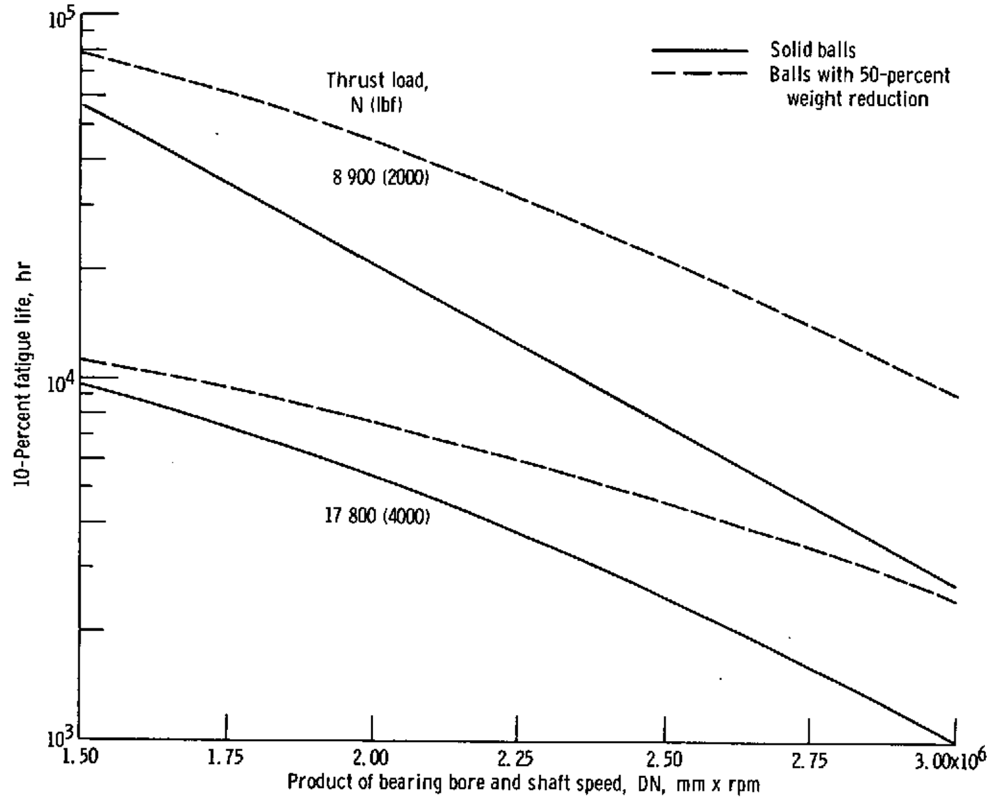

Figure 1. - Theoretical fatigue life of a 150-millimeter-bore ball bearing with solid balls and with balls having 50-percent weight reduction for two thrust loads. (Based on analysis of ref. 2.)

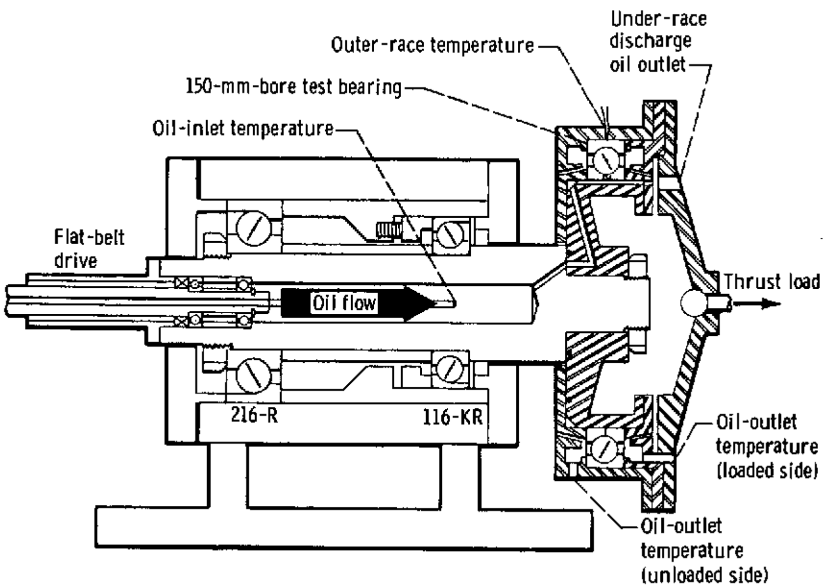

Figure 2. - Schematic of three-bearing test spindle.

(a) Solid ball bearing.

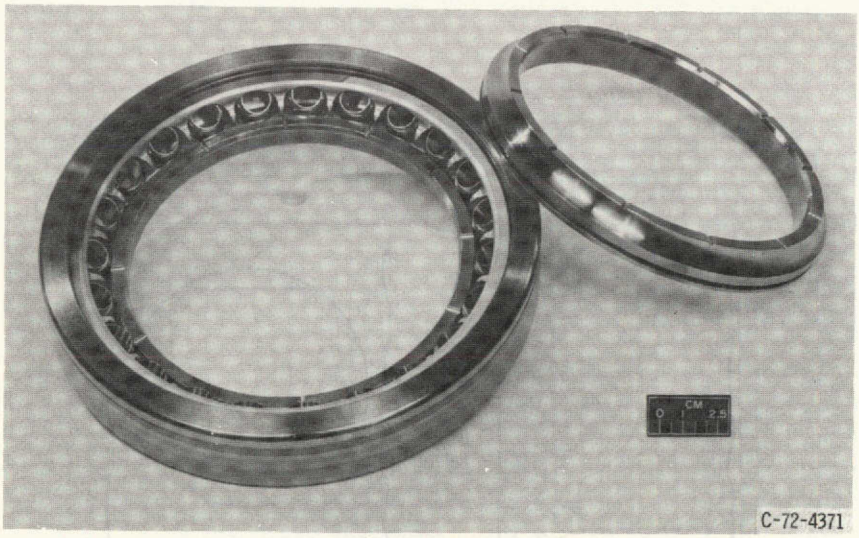

(b) Drilled ball bearing.

Figure 3. - Test bearing. Type - angular contact, split inner race; material - AISI M-50 tool steel; cage type - one-piece machined, outer-race located.

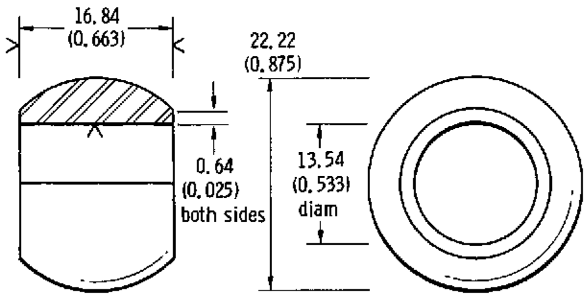

Figure 4. - Details of drilled-ball design. (Dimensions are in mm (in.). Surface finish is 0.4 μm (16μ in.) where marked by ∨.)

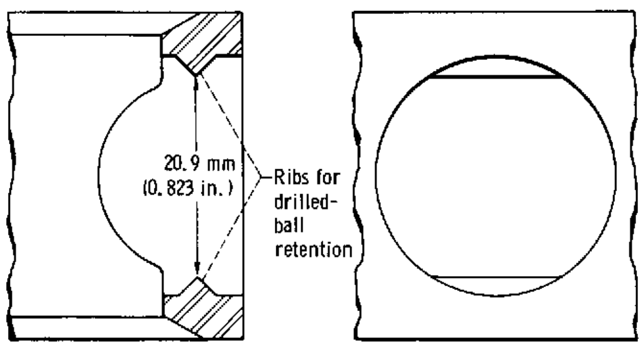

Figure 5. - Details of drilled-ball cage modification.

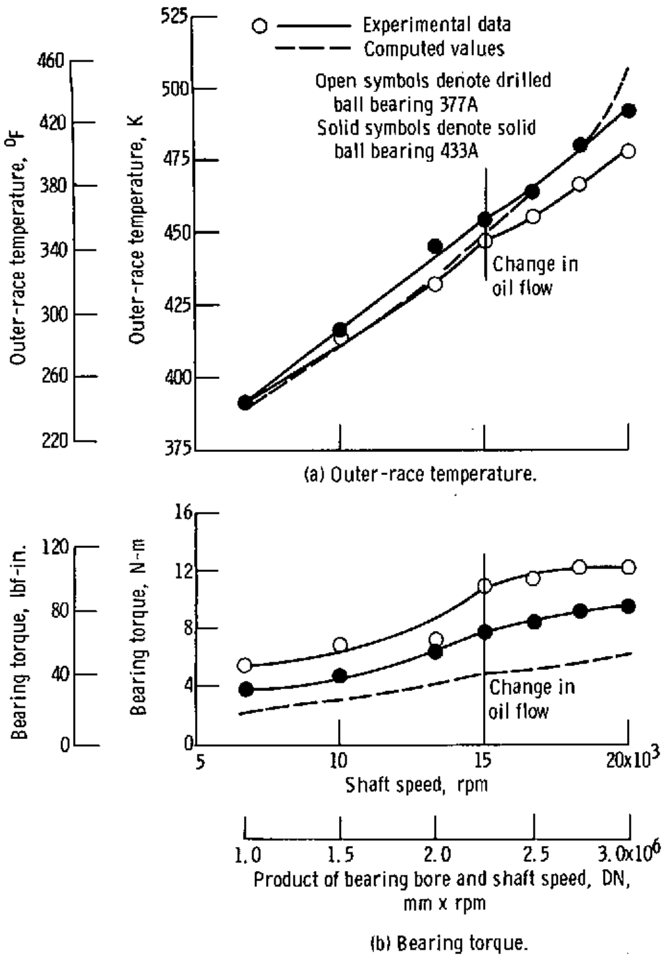

Figure 6. - Comparison of solid and drilled ball bearing outer-race temperature and torque as a function of shaft speed at 8900-newton (2000-lbf) thrust load. Lubricant, MIL-L-23699 at 367 K (200° F) oil-inlet temperature; oil flow, 4.35×10^{-3} and 5.80×10^{-3} cubic meter per minute (1.15 and 1.53 gal/min).

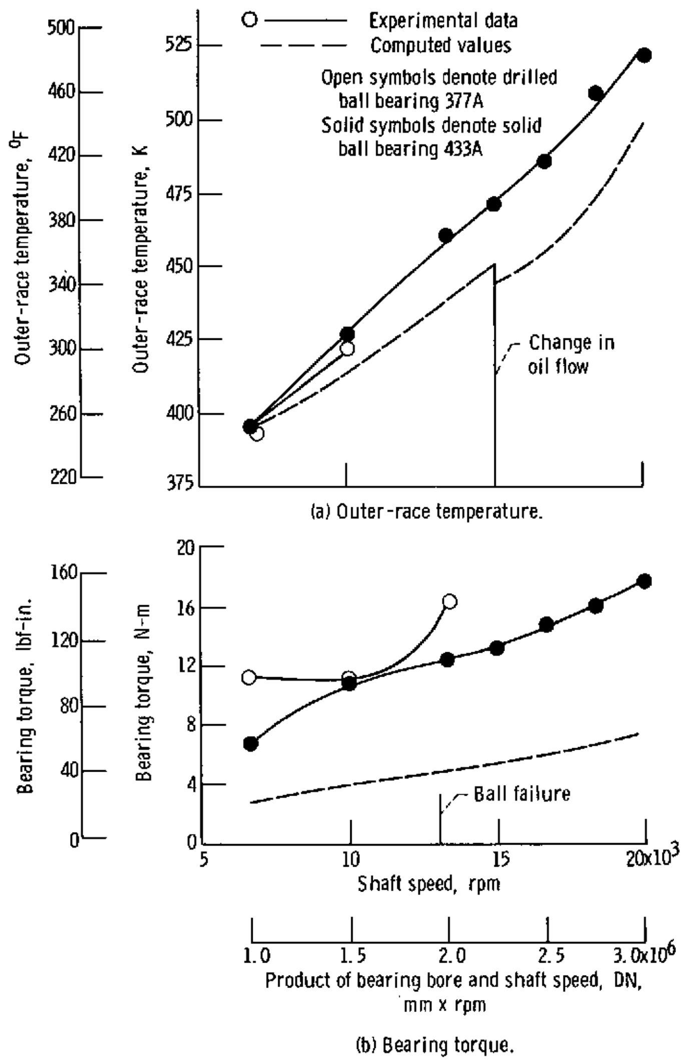

Figure 7. - Comparison of solid and drilled ball bearing outer-race temperature and torque as a function of shaft speed at 17 800-newton (4000-lbf) thrust load. Lubricant, MIL-L-23699 at 367 K (200° F) oil-inlet temperature; oil flow, 4.35×10^{-3} and 5.80×10^{-3} cubic meter per minute (1.15 and 1.53 gal/min).

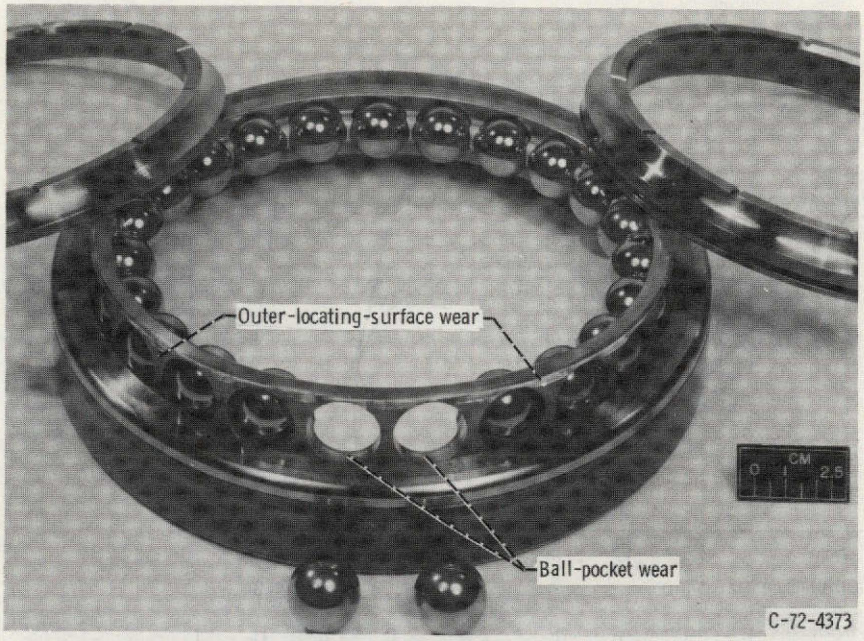

Figure 8. - Solid ball bearing 433A after 17 800-newton (4000-lbf) thrust load run at speeds from 6670 to 20 000 rpm (1 million to 3 million DN), showing ball-pocket and outer-locating-surface cage wear.

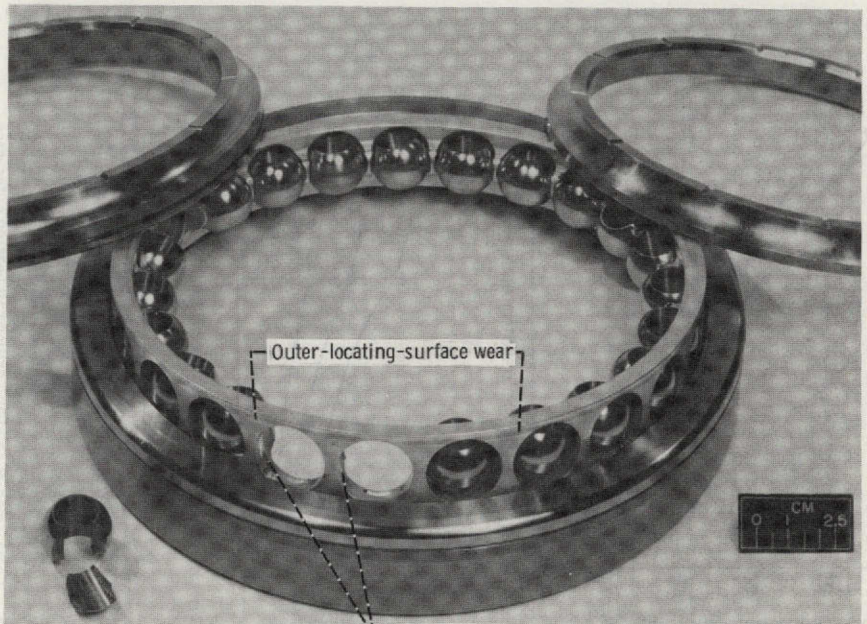

Figure 9. - Drilled ball bearing 377A after 17 800-newton (4000-lbf) thrust load run at speeds from 6670 to 13 000 rpm (1 million to 2 million DN), showing ball-pocket and outer-locating-surface cage wear. (Ball fractured at 13 000 rpm.)

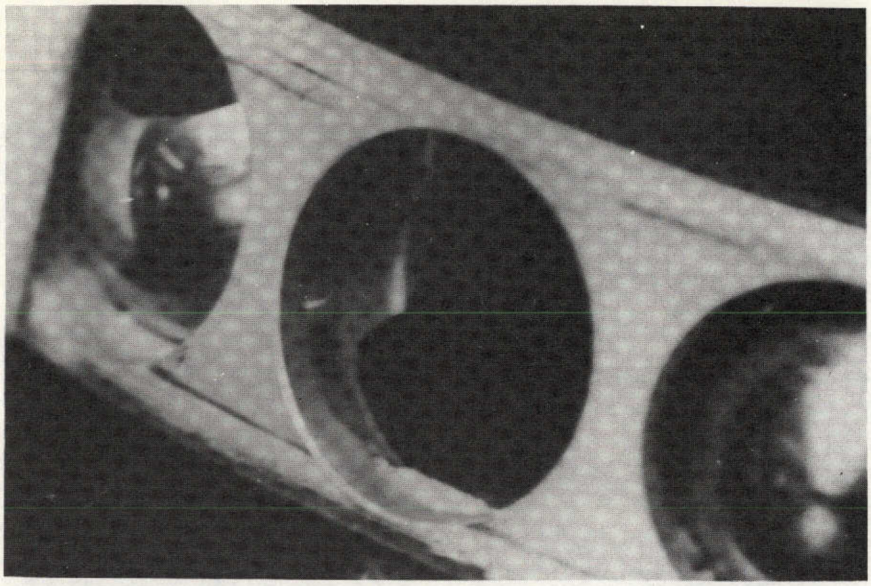

Figure 10. - Portion of cage from drilled ball bearing 377A after 17 800-newton (4000-lbf) thrust load test.

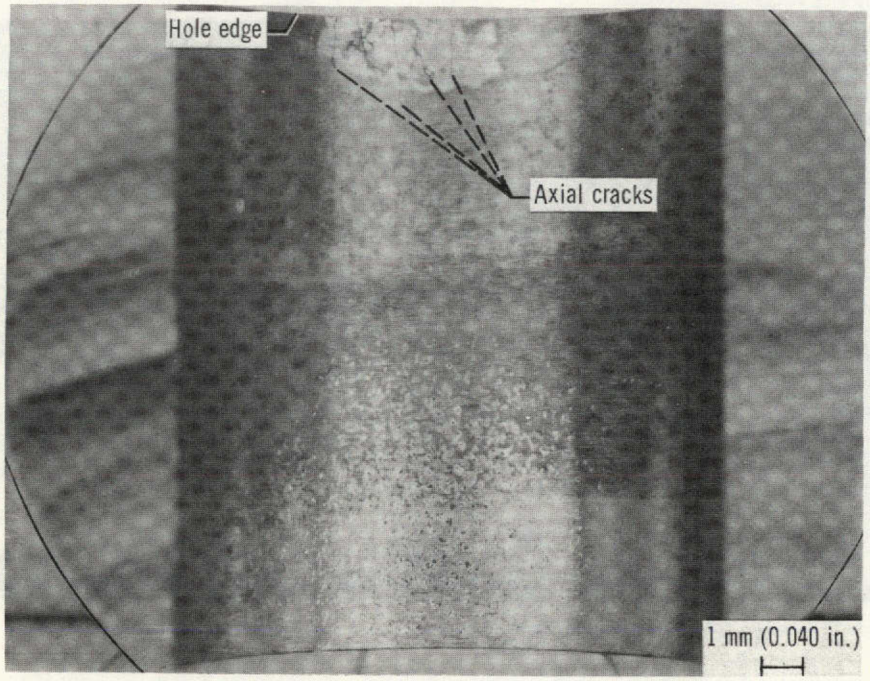

Figure 11. - Half section of drilled ball from bearing 377A, showing pitted hole surface and axial cracks near hole edge.

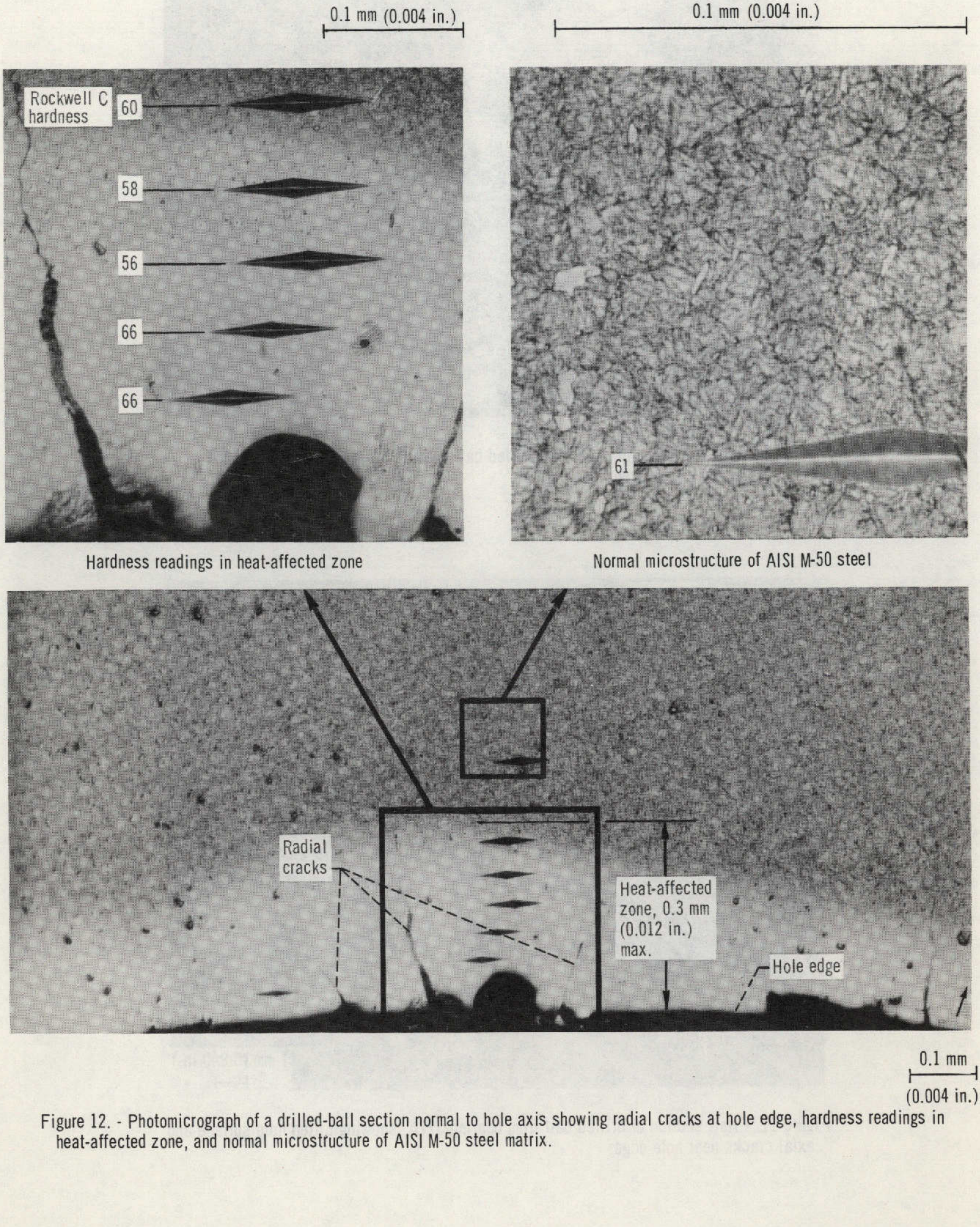

Figure 12. - Photomicrograph of a drilled-ball section normal to hole axis showing radial cracks at hole edge, hardness readings in heat-affected zone, and normal microstructure of AISI M-50 steel matrix.

NASA-Langley, 1974 E-7722